Power Distribution Systems Failure Response Against Extreme Events: a Stochastic Approach

Henrique O. Caetano * **Luiz Desuó N.** * **Matheus S. S. Fogliatto** * **Carlos D. Maciel** *

* *Department of Electrical and Computing Engineering - São Carlos School of Engineering University of São Paulo - São Carlos, SP, Brazil. (e-mail: henriquecaetano1@usp.br carlos.maciel@usp.br*

Abstract: Power Distribution Systems are a critical infrastructure, and there is a growing interest related to their capacity to deliver and maintain power supply to the final customer. In this sense, the failure response of a typical Distribution System (DS) must be correctly assessed, especially when considering Low Frequency, High Impact (LFHI) events, such as extreme weather scenarios. Previous studies focus on topological and qualitative approaches, thus not considering the impact of extreme weather on the DS's reliability metrics related to the frequency and duration of the failure. In this work, a fragility curve model was used to sample time until failure and time to repair inside a daily time window of a real Brazilian DS while taking weather variables into account. The Monte Carlo method was used to verify both power flow parameters and weather variables' influence on the frequency and duration of failures. A gradual node removal approach was also modelled to investigate the impact of energy not supplied. Results show that the weather variables values can drastically change the failure response of the DS in both the time window and node removal approaches. Furthermore, when considering redundancy (alternative energy paths), in the most extreme weather scenario, an increase in system redundancy did not improve failure response, contrary to what is expected. In this sense, an extreme weather failure response analysis is recommended in any investment study related to a DS - such as switch or protective device placement.

Keywords: Power Distribution System; Resilience; Survival Analysis; Extreme Weather Events; Reliability Metrics; Monte Carlo Simulation

1. INTRODUCTION

Electrical Power Systems (EPS) is considered one of the most important critical infrastructures (CI) where its continuity performance index is the subject of several pieces of research (Yusta et al., 2011). It is possible to define a failure in a typical DS as any abnormal condition in the system that leads to an electrical failure in given equipment (such as transformers, generators and buses), which can further lead to loss of energy supplied to the final consumes (Shen et al., 2021). Most of the power outages experienced by the customers are specifically in the Distribution Systems (DS) sector (Gómez-Expósito et al., 2018), which is responsible for making the ultimate connection with the customers. Consequently, DS failure response is the object of several studies, particularly in understanding how internal and external factors can cause interruptions/failures in the DS (Shen et al., 2021). This comprehension can further be used to improve the structure of the system itself, in areas such as planning, updating and expansion of power systems (Afzal et al., 2020).

⋆ This work was partially fomented by São Paulo Research Foundation(FAPESP), grant 2021/12220-1, 2019/06531-4 and 2014/50851-0, CNPq 465755/2014-3, BPE Fapesp 2018/19150-6 and CAPES - Brazil.

Since the placement of DSs is usually in large areas, external factors can influence their failure response. As an example, extreme weather events constitute one of the leading causes of failures in the DS (Jufri et al., 2019). They are categorized as Low Frequency, High Impact (LFHI) events, which despite happening with a low degree of frequency, can cause a significant level of disruption. When assessing the failure response of Distribution Systems, the consideration of LFHI is essential to understand further its impact on the continuity of power delivered. Two factors are significant regarding DSs failure response: failure frequency, regarding how many disruptions happened in a given time interval, and failure duration related to the total needed time to restore electrical energy to out-of-service customers. The minimization of both factors is of extreme importance, allowing the utility to avoid higher fines, as well as to assure power continuity at global and individual levels (Heydt, 2010).

In that regard, for a given failure in a DS, it is often important to know how long it took for it to happen (time to failure) and how long the system will take to recover itself (time to repair) (Bessani et al., 2016). Moreover, for a better understanding of failure frequency in DSs, recent studies separate the failure into groups (coupling together similar causes), including extreme weather events (Fogliatto et al., 2020; Jufri et al., 2019).

Regarding the impact of extreme weather events on the failure response of DSs, the work done by (Bessani et al., 2019) focuses on the probabilistic assessment of power systems under extreme weather scenarios. The authors use failure history data and Monte Carlo Simulations to create fragility curves for the failure and repair models and a stochastic approach to address the frequency and duration of failures in a DS. In (Bessani et al., 2018), the authors apply a multi-agent simulation over a power distribution network, with the primary goal of enhancing system robustness by opening/closing switches between nodes. The authors in (Fogliatto et al., 2020) distinct different causes of failures in a DS, including a model for addressing the repair time in function of various environmental variables (such as temperature, wind speed and precipitation level).

On the other hand, from a vulnerability analysis point of view, the works above do not consider the particularity of extreme weather events. The possible influence of weather variables on the failure rate and repair time of each component, for example, is ignored. Additionally, for each extreme weather scenario, the reliability metrics related to frequency and duration of failures for both the final customer and the whole system (Heydt, 2010) must be calculated. Previous works neglect that, thus failing to address and differentiate the impact of each failure in the DS power continuity.

Additionally, the collective impact of system redundancy (in terms of alternative connections and switches available), load demand and feeder capacity on the failure response of extreme weather events are neglected in previous works, despite their importance to the system (Hilbers et al., 2021; Jordehi, 2018). Finally, despite the development of curves related to the time until failure and the time to repair DS components, they are yet to be tested as a scenario generator model in a failure response analysis of a real distribution system.

This paper develops a Monte Carlo Simulation (MCS) approach based on time windows. The main goal is to directly use fragility curves models for the time until failure and the time to repair in a real-life DS. We consider the impact of extreme weather events by using different curves based on weather intensity. Furthermore, the effect of load demand and feeder power capacity variation in extreme weather scenarios is done by simulating node removal failures. Lastly, reliability metrics, such as the Customer Average Interruption Frequency Index (CAIFI), are calculated for each iteration of the MCS while varying redundancy - in the form of normally open switches - and weather intensity.

The main gaps to be filled by this work are:

- A MCS model for extreme weather events in DS that can take into consideration the extreme weather variables (such as precipitation level) directly into the fragility curve;
- The calculation of reliability metrics related to the frequency and duration of failures, which can be used to determine the impact of extreme weather events on the continuity of energy supply to the customer;
- The variation of redundancy, load demand and feeder power capacity, and how these variations can affect the failure response in extreme weather scenarios.

The paper is organized as follows: The proposed failure response model is presented in Section 2, encompassing the Reliability Metrics, the Monte Carlo Simulation, and the time window model. We present and discuss the results in Section 3. Lastly, conclusions are stated in Section 4.

2. MATERIALS AND METHODS

The real Brazilian DS represented in Figure 1 was used for all simulation in this work, to properly show the scalability of the model. Additionally, the work done in (Fogliatto et al., 2020) took failure data from the mentioned DS and used it to create distribution curves regarding both the time until failure and the repair time.

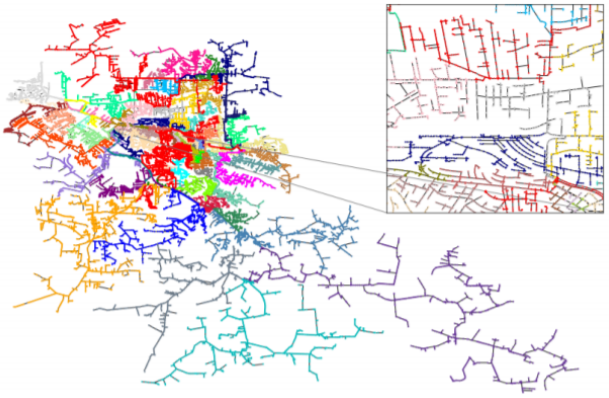

Figure 1. Real DS of a Brazilian city used in all simulations. The system has over 40000 bars, 3800 switches and 36000 switches. The subfigure zooms in a subsection of the system, for an enhanced view of its topology. Each color represents a different substation. Source: Fogliatto et al. (2022).

Regarding the time until failure, the Weibull model developed in (Fogliatto et al., 2020) was used, where the final distribution curve take into consideration the following weather variables:

- daily number of atmospheric discharge,
- wind speed (km/h)
- maximum daily temperature (in C^o)
- minimum temperature (in C^o)
- precipitation level (mm/h)
- air relative humidity (%)

With that in mind, in order to bring the influence of extreme weather events to the proposed methodology, three scenarios were sampled for the time until failure, as shown in Fig. 2. Each failure mode represents the distribution curve when the minimum, average or maximum values of each weather variables is used, to properly model different failure intensities. With this method, it was possible to develop three scenarios for the time until failure curve, each one representing a different level of weather intensity.

On the other hand, the distribution curve related to the time to repair was also developed in (Fogliatto et al., 2020), for different causes of failures. Since this work aims to analyse the impact of extreme weathers into DSs, only the atmospheric curve was used, as shown in Fig. 3.

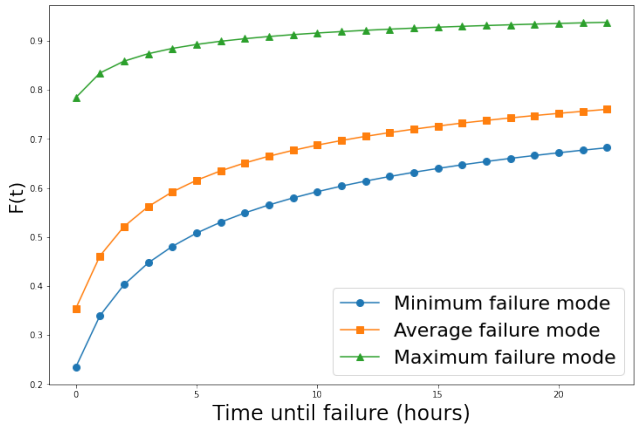

Figure 2. Cumulative distribution function for the time until failure (or lifetime), in hours, representing the time period between two consecutive failures for a given node in the network. Failure mode depends on weather variables, and affects network resilience. The failure modes represents the weather intensity, from least intense (minimum) to most intense (maximum).

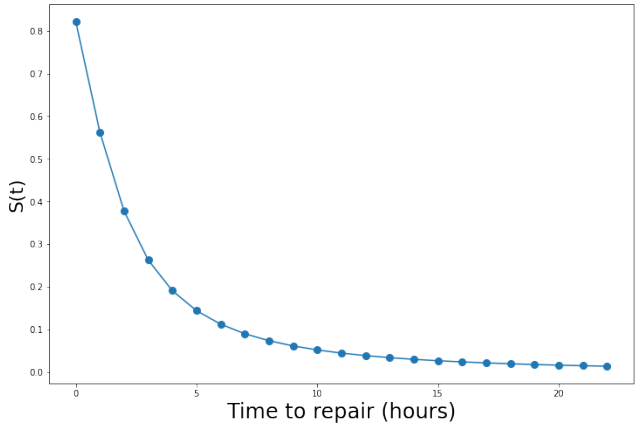

Figure 3. Distribution function for the time to repair of the SD used, representing the time to address the process of failure detection, isolation and system restoration. In this case, only atmospheric failures were considered, to directly assess the impact of extreme weathers into the simulations.

Another aspect to be considered is the system redundancy. In this work, the redundancy indicates the percentage of connections (lines or switches) that are used in the network, in comparison to all possible combinations. For a given value of redundancy r (between 0 and 1), $(1-r)$ lines are randomly removed, an approach already used in previous works (Quattrociocchi et al., 2014). The analysis of the redundancy is crucial to correctly assess the DS failure response, since the addition of new lines on the system can be economically costly, and must be carefully done (Heydt, 2010). In this work, three values of redundancy were used: 80%, 90% and 100%, representing typical values of redundancy in real life DSs (Rodrigues Mendes Ribeiro et al., 2019).

Additionally, two parameters related to power flow were used in the full simulation model. The feeder capacity tolerance α is shown in Eq. 1, where $P_{0,f}$ is the nominal distribution capacity, in terms of active power, of feeder f and P_f is the actual demand of feeder. In this sense, an increase in the α parameter represents an elevation of the active power of a feeder, which can be used to restore additional customers in the case of power transfer between feeders.

$$P_f = (1+\alpha) \cdot P_{0,f} \tag{1}$$

The other parameter used in the power flow was the load multiplicative factor β, represented in Eq. 2. In this case, $L_{0,c}$ is the expected active power demand of customer c, and L_c is the actual active power, based on the β parameter. A higher β value represents the increase of power demand in the DS.

$$L_c = (1+\beta) \cdot L_{0,c} \tag{2}$$

Lastly, for all simulations, the DC Power Flow model (Purchala et al., 2005) was used to properly assess topological and electrical constraints, such as maximum line current, maximum bus voltage and maximum load active power into the full failure response model.

2.1 Reliability Metrics

In the context of DSs, the continuity of power delivery to the final customers is one of the most important fact to be considered. In this regard, this aspect is usually measured through standard reliability metrics (Heydt, 2010). In this work, four reliability metrics were used:

- System Average Interruption Frequency Index (SAIFI), related to the expected number of failures a given customer suffers in a given time window (interruptions/(customers*time)), calculated as shown in Eq. 3, where N_i is the number of customers affected by a single failure (i), and N_T is the total number of customers in the system.

$$SAIFI = \frac{\sum_i N_i}{N_T} \tag{3}$$

- System Average Interruption Duration Index (SAIDI), which shows the expected duration of failures for a given customer in the DS, calculated by Eq. 4, where r_i is the repair time of failure i. In this work, the values sampled from the curves shown in Figs. 2 and 3, as detailed later on.

$$SAIDI = \frac{\sum_i N_i r_i}{N_T} \tag{4}$$

- Customer Average Interruption Frequency Index (CAIFI), that is concerned with the average frequency of failures for customers that are being affected by failures. This metric is calculated in Eq. 5, where N_c is the number of customers that suffered from any failure during the time window.

$$CAIFI = \frac{\sum_i N_i}{N_c} \tag{5}$$

- Customer Average Interruption Duration Index (CAIDI), representing the expected duration of a failure that affected a given customer (minutes/failure), as shown in Eq. 6

$$CAIDI = \frac{\sum_i N_i r_i}{\sum_i N_i} = \frac{SAIDI}{SAIFI} \tag{6}$$

And the last metric used in this work, that takes into consideration the power flor particularities of the DS, is the Energy Not Supplied (ENS), as shown in Eq. 7, where the active power of each customer in failure, L_c is multiplied by the repair time, r_i, to give the total energy not supplied in the considered time window.

$$ENS = \sum_i \sum_{N_i} L_c r_i \tag{7}$$

2.2 Monte Carlo Simulation (MCS)

The full flowchart of the Monte Carlo Simulation method used in this work is presented in Fig. 4. The initial step is to set the failure scenario, by choosing a curve between the ones presented in Fig. 2. After the scenario is fixed, the next step is to run N iterations, where N = 100 was used in this work. For each iteration, the time until failure and time to repair are sampled from Figs. 2 and 3, respectively, and are used to define the status of each customer during the time window. For example, if node i has tf = 3 (in hours) and tr = 5 (in hours), then all customers affected by the failure will be disconnected from the DS for the time interval between t=3 and t=8. Since the time window is T = 24 hours, any node with $tf > 24$ will not be affected. Lastly, after a iteration is finished, the status of each customer over time is used to calculate each reliability metric showed in Subsection 2.1

The possibility of node removal was also considered in this work, where the Monte Carlo method was repeated, but this time, different values for the power flow parameters (α and β) have been chosen, and the nodes were gradually removed from the network, while calculating the ratio of Energy Not Supplied (in comparison to the total demand of the system) after each removal.

3. RESULTS AND DISCUSSION

Figs. 5 and 6 show the simulation results, where the Monte Carlo method was applied, with N=100 iterations, and a box plot was generated to show the range and the overall distribution of reliability metrics values along each iteration. All possible values of failure mode and redundancy (r) were taken into consideration, summing up 9 possible scenarios. For all simulations, the value of the power flow variables, α and β, were fixed at 0, meaning that the initial DS was used without any further modifications. This was done to properly analyse the impact of extreme weather scenarios in typical situations regarding both load demand and feeder capacity.

At Fig. 5, it is possible to analyse the expected duration of failures, both at system (global) as well as customer (local) levels. In this regard, for minimum and average failure modes, the mean value of SAIDI and CAIFI decreases with the increase of redundancy, showing a better failure response with the increase of alternative connections at the network. This result is expected in the literature, since the increase of system redundancy is usually done to enhance its failure response, especially in electrical power systems,

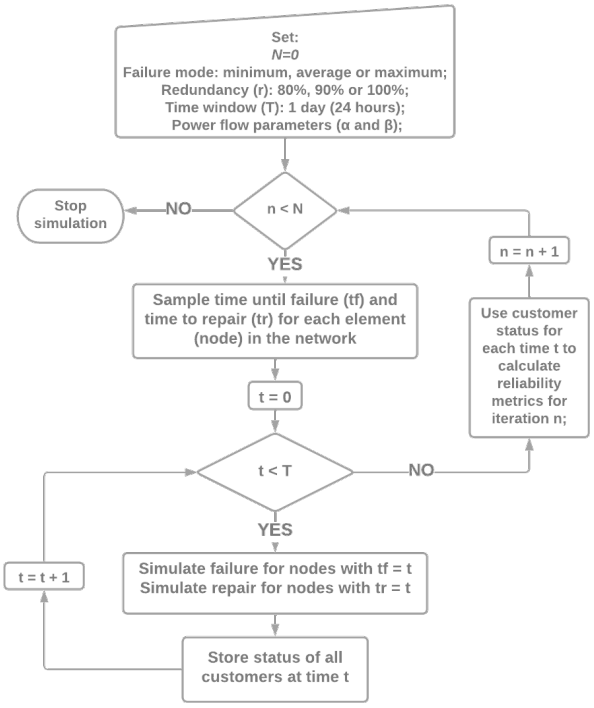

Figure 4. Full Monte Carlo Simulation (MCS) flowchart. After a extreme weather event scenario is set, N MCS iterations are simulated, with a given time window T (in hours). Fragility curves are used to set the time until failure and time to repair of each element in the network, and different reliability metrics are calculated at the end of each MCS iteration.

as shown in (Rodrigues Mendes Ribeiro et al., 2019) and (Quattrociocchi et al., 2014), for example.

For the maximum failure mode, however, the mean value of SAIDI and CAIDI do not change abruptly with changes in redundancy, and the confidence intervals intersect, thus not being possible to distinguish considerable improvements in system response to failures with the increase in redundancy. This result show that an increase in redundancy may not improve system failure response, at least when considering an extreme weather event scenario (since the maximum failure mode represents the most extreme weather variables).

In Fig. 6, the boxplot of SAIFI shows the same pattern describe above, meaning that the addition of redundancy can enhance the DS failure response for minimum and average failure mode, but not for the maximum failure mode scenario. Lastly, CAIDI remained constant, since its calculation, done by Eq. 6, is done using only the time to repair, which is sampled from the distribution curve of Fig. 3, and consequently is independent of failure mode, and doesn't have abrupt changes related to redundancy variation.

It is important to notice that the addition of redundancy in a DS (through line and switch allocation) usually requires economical and technological investments by the DS utility (Shahbazian et al., 2020). In this sense, a return of such investment, in the form of failure response enhancement, is expected. The results presented here show

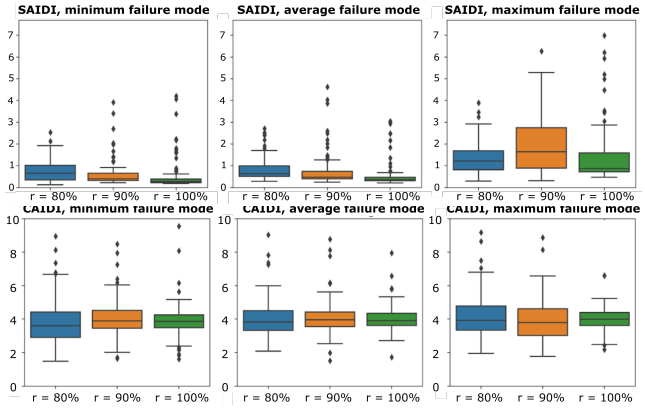

Figure 5. Boxplot for the Average Interruption Duration Index, both for the system (SAIDI) and for the Customer (CAIDI), varying failure mode and redundancy (r). In all cases, $\alpha = 0$ and $\beta = 0$

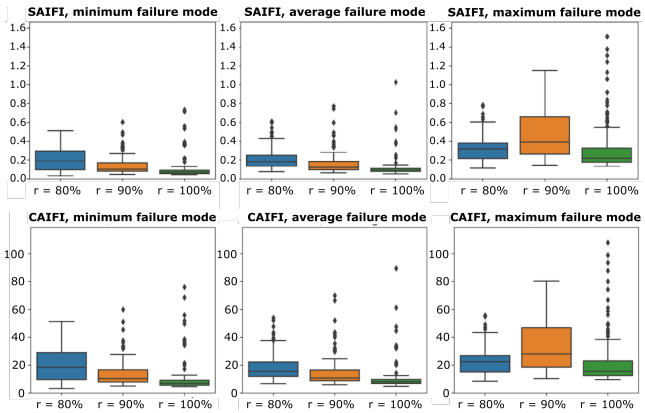

Figure 6. Boxplot for the Average Interruption Frequency Index, both for the system (SAIFI) and for the Customer (CAIFI), varying failure mode (related to extreme weather intensity) and redundancy (r). In all cases, $\alpha = 0$ and $\beta = 0$

that this may not be the case, especially when considering extreme weather scenarios. In this sense, in any investment study of a DS, there must be done an extensive analysis regarding the influence of external factors (such as weather variables), to properly understand their influence in the DS failure response.

The results related to gradually node removal are shown in Figs. 7 and 8. Each horizontal line shows the minimum ratio of removed nodes (between all 5 curves, in each Figure) in the DS necessary to achieve 25%, 50% and 75% of energy not supplied (ENS).As it can be seen in Figure 7, the distinction between each curve is stronger for the first removed nodes, particularly before 25% ENS is achieved. After that, all curves tend to converge to the same behavior. This result is expected, since the only difference between each curve is the load demand (as set by the β parameter in Eq. 2), and thus, since no topological distinctions are made, when multiple nodes are removed, the system is unable to transfer loads between feeders, and collapses regardless of the power flow parameters.

Regarding variations in feeder capacity, in Figure 8, it is possible to observe that once again, all curves tend

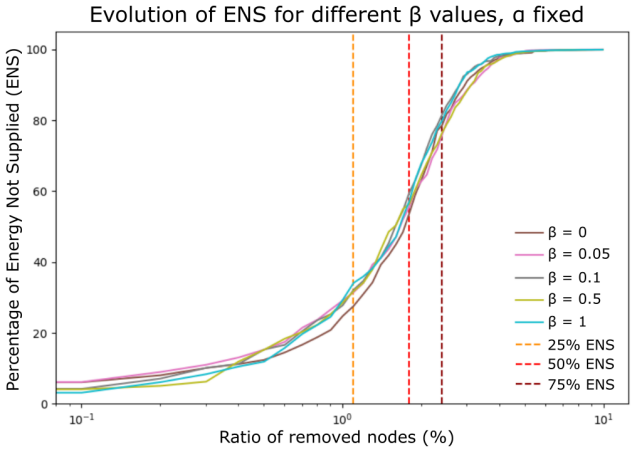

Figure 7. Evolution of the Energy Not Supplied (ENS) values for the DS, when gradually removing one node at a time. In this case, different values of β were applied, while maintaining $\alpha = 0$ fixed. The horizontal lines represents the minimum ratio of nodes, between all 5 β values, necessary to achieve each critical ENS level (25%, 50% and 75%).

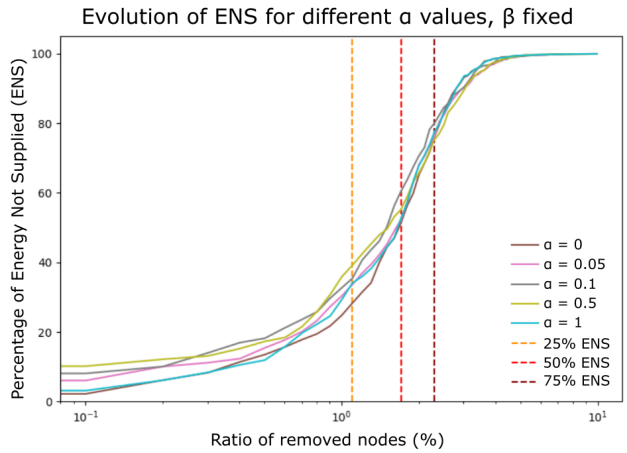

Figure 8. Evolution of the Energy Not Supplied (ENS) values for the DS, when gradually removing one node at a time. In this case, different values of α were applied, while maintaining $\beta = 0$ fixed. The horizontal lines represents the minimum ratio of nodes, between all 5 α values, necessary to achieve each critical ENS level (25%, 50% and 75%).

to approach each other as the ratio of removed nodes increases. It is possible to observe, however, a slightly higher distinction between the curves, for ENS values lower than 50%, if compared to the curves presented in Fig. 7. This behavior shows how the possibility of transferring nodes between feeders - that is only possible with higher values of α, representing the power tolerance - can enhance the DS failure response, even when considering a time window related to extreme weather scenarios.

Additionally, Table 1 shows, for each pair of (α, β), the ratio of removed nodes in the DS necessary to achieve 25%, 50% and 75% of energy not supplied (ENS), which are represented by the variables $ENS_{25\%}$, $ENS_{50\%}$ and $ENS_{75\%}$, respectively. the lowest value achieved for each

critical value is highlighted, showing the optimal pair of power flow parameters for the DS simulated. The highlighted values represents the highest ratio of nodes necessary to achieve all three of the critical energy not supplied values, which are further shown in Table 2.

It is possible to observe how, for each critical ENS values, different values of α and β showed the best failure system response. The tuple ($\alpha = 0, \beta = 1$), for example, is the best result regarding a 25% critical level of ENS. On the other hand, the same configuration led to a 2.17 ± 0.89 ratio of removed nodes necessary to achieve the 75% level of ENS, which is high if compared to the value achieved for other tuple configurations. In this sense, the power flow parameters (α and β) must be taken into consideration when modeling the failure response of DS against extreme weather events, leading to a better understanding of the complete system dynamic.

Table 1. Mean and variance values for the ratio of removed nodes necessary to reach 3 different critical levels of Energy Not Supplied (ENS) in the DS simulated: 25%, 50% and 75%, as shown in $ENS_{25\%}$, $ENS_{50\%}$ and $ENS_{75\%}$, respectively. The failure mode was fixed as average, and the redundancy was fixed at $r = 100\%$.

$\alpha = \mathbf{0}$

β	$\mathbf{ENS_{25\%}}$	$\mathbf{ENS_{50\%}}$	$\mathbf{ENS_{75\%}}$
0	1.31±0.49	1.73±0.79	1.93±1.0
0.05	1.32±0.49	1.84±0.83	2.07±1.08
0.1	1.32±0.48	1.81±0.76	2.07±0.99
0.5	1.4±0.44	1.88±0.71	2.25±1.05
1	$\mathbf{1.41 \pm 0.40}$	1.89±0.66	2.17±0.89

$\alpha = \mathbf{0.05}$

β	$\mathbf{ENS_{25\%}}$	$\mathbf{ENS_{50\%}}$	$\mathbf{ENS_{75\%}}$
0	1.34±0.47	1.76±0.76	2.0±1.01
0.05	1.37±0.41	1.86±0.66	2.09±0.88
0.1	1.43±0.43	1.92±0.71	2.21±0.93
0.5	1.39±0.46	1.92±0.72	$\mathbf{2.32 \pm 1.10}$
1	1.33±0.47	1.85±0.77	2.17±1.1

$\alpha = \mathbf{0.1}$

β	$\mathbf{ENS_{25\%}}$	$\mathbf{ENS_{50\%}}$	$\mathbf{ENS_{75\%}}$
0	1.31±0.39	1.80±0.73	2.05±1
0.05	1.34±0.41	1.85±0.7	2.15±1.04
0.1	1.30±0.43	1.75±0.43	1.97±0.96
0.5	1.33±0.48	1.79±0.79	2.05±1.03
1	1.28±0.50	1.70 ± 0.77	1.99±1.07

$\alpha = \mathbf{0.5}$

β	$\mathbf{ENS_{25\%}}$	$\mathbf{ENS_{50\%}}$	$\mathbf{ENS_{75\%}}$
0	1.35±0.42	1.87±0.71	2.2±1.01
0.05	1.29±0.5	1.76±0.81	1.99±1.05
0.1	1.30±0.50	1.72±0.79	1.91 ± 1.01
0.5	1.39±0.48	$\mathbf{1.95 \pm 0.76}$	2.31±1.05
1	1.26 ± 0.49	1.76±0.81	2.12±1.12

$\alpha = \mathbf{1.0}$

β	$\mathbf{ENS_{25\%}}$	$\mathbf{ENS_{50\%}}$	$\mathbf{ENS_{75\%}}$
0	1.42±0.43	1.93±0.70	2.23±0.97
0.05	1.34±0.47	1.88±0.75	2.27±1.09
0.1	1.35±0.43	1.85±0.74	2.06±0.95
0.5	1.36±0.42	1.87±0.75	2.22±1.06
1	1.38±0.42	1.85±0.69	2.06±0.89

Table 2. Best DS scenario related to 3 critical Energy Not Supplied (ENS) values. In each case, the highest ratio of removed nodes necessary to achieve the critical level was computed, together with the respective combination of α and β (power flow parameters, as shown in Eq. 1 and 2, respectively).

Critical ENS Level	Ratio of removed nodes	α	β
25%	1.41 ± 0.4	0	1
50%	1.95 ± 0.76	0.5	0.5
75%	2.32 ± 1.1	0.05	0.5

This work aimed to apply fragility curves related to time until failure and repair time of a DS into a complete failure response model while also considering extreme weather variables. Previous works did not consider the direct impact of extreme weather events on the failure response of a DS. The results presented in Figs. 5 and 6, for example, would be compiled into a single Boxplot, thus neglecting the discrepancy between each weather scenario, which could lead to misleading results regarding any short or long term investment analysis of a DS.

Additionally, the variation of power flow restrictions, which are represented in this work by parameters α and β, is usually not applied in the face of extreme weather scenarios in the literature. By doing so in this work, it was possible to verify how the optimal values of the restrictions above change in the face of a given extreme weather scenario, as highlighted in Table 2. A DS operator can use this approach in the face of historical failure data by simulating each failure scenario using the proposed methodology and finding the optimal values of α and β in each case, which can be further applied to the real DS, enhancing its failure response.

With the application of extreme weather uncertainties, coupled with the Monte Carlo method, as well as a time window approach, it was possible to go one step further into the failure response problem of DS by considering the stochasticity of the final complete model while also calculating different reliability metrics related to the frequency and duration of failures. Additionally, the methodology presented can be extended to assess any failure model of a typical Distribution System by adequately adjusting the distribution curves, depending on the availability of historical data and expert knowledge.

4. CONCLUSION

This paper presents an Electrical Distribution System failure response analysis against extreme weather events using the time until failure and the time to repair each element in the network as random variables with individual distribution curves. The Monte Carlo method is applied, coupled with a time window model, while also calculating different reliability metrics related to failure frequency and duration.

It was possible to model both external (weather environment) and internal (redundancy, load demand and feeder power capacity) factors while analysing the DS failure response in each case. It was possible to observe how the extreme weather intensity can drastically change the DS behaviour, especially when considering possible vari-

ations in internal and external factors. Furthermore, the results emphasise the importance of incorporating extreme weather variables into the DS failure response model to enhance further the DS operator's possible short and long-term decisions.

Additionally, the complete simulation model presented in this work can be used to properly assess failure related to extreme weather events into topological and economic problems related to Electrical Power systems, such as the Optimal Allocation of protective and controlling devices. In this case, the reliability metrics can be used as an objective function optimised. Future works should introduce attacks in the response model to compare with random failures; introduce additional curves related to the failure and repair model (related to different causes of failures); and use other metrics, such as centrality and connectivity, to properly assess the DS failure response.

REFERENCES

Afzal, S., Mokhlis, H., Illias, H.A., Mansor, N.N., and Shareef, H. (2020). State-of-the-art review on power system resilience and assessment techniques. *IET Generation, Transmission & Distribution*, 14(25), 6107–6121. doi:https://doi.org/10.1049/iet-gtd.2020.0531. URL `https://ietresearch.onlinelibrary.wiley.com/doi/abs/10.1049/iet-gtd.2020.0531`.

Bessani, M., Ribeiro, R.R.M., Pagani, G.A., Aiello, M., and Maciel, C.D. (2018). Robustness of reconfigurable complex systems by a multi-agent simulation: Application on power distribution systems. In *2018 Annual IEEE International Systems Conference (SysCon)*, 1–6. doi:10.1109/SYSCON.2018.8369553.

Bessani, M., Fanucchi, R., Achcar, J., and Maciel, C. (2016). A statistical analysis and modeling of repair data from a brazilian power distribution system. doi:10.1109/ICHQP.2016.7783446.

Bessani, M., Massignan, J.A.D., Fanucchi, R.Z., Camillo, M.H.M., London, J.B.A., Delbem, A.C.B., and Maciel, C.D. (2019). Probabilistic assessment of power distribution systems resilience under extreme weather. *IEEE Systems Journal*, 13(2), 1747–1756. doi:10.1109/JSYST.2018.2853554.

Fogliatto, M., Maciel, C., Ribeiro, R., Bessani, M., London Jr, J., Desuó, L., and Santos, T. (2020). Time to event analysis for failure causes in electrical power distribution systems. doi:10.48011/asba.v2i1.1662.

Fogliatto, M.S.S., N., L.D., Ribeiro, R.R.M., Monteiro, J.R.B.A., London, J.B.A., Bessani, M., and Maciel, C.D. (2022). Lifetime study of electrical power distribution systems failures. *Journal of Control, Automation and Electrical Systems*. doi:10.1007/s40313-021-00888-6. URL `https://doi.org/10.1007/s40313-021-00888-6`.

Gómez-Expósito, A., Conejo, A.J., and Cañizares, C. (2018). *Electric energy systems: analysis and operation (2nd ed.)*. CRC press. doi:https://doi.org/10.1201/9781315192246.

Heydt, G.T. (2010). The next generation of power distribution systems. *IEEE Transactions on Smart Grid*, 1(3), 225–235. doi:10.1109/TSG.2010.2080328.

Hilbers, A., Brayshaw, D., and Gandy, A. (2021). Efficient quantification of the impact of demand and weather uncertainty in power system models. *IEEE Transactions on Power Systems*, 36(3), 1771–1779. doi:10.1109/TPWRS.2020.3031187.

Jordehi, A.R. (2018). How to deal with uncertainties in electric power systems? a review. *Renewable and Sustainable Energy Reviews*, 96, 145–155. doi:https://doi.org/10.1016/j.rser.2018.07.056. URL `https://www.sciencedirect.com/science/article/pii/S1364032118305641`.

Jufri, F.H., Widiputra, V., and Jung, J. (2019). State-of-the-art review on power grid resilience to extreme weather events: Definitions, frameworks, quantitative assessment methodologies, and enhancement strategies. *Applied energy*, 239, 1049–1065.

Purchala, K., Meeus, L., Dommelen, D., and Belmans, R. (2005). Usefulness of dc power flow for active power flow analysis. volume 1, 454 – 459 Vol. 1. doi:10.1109/PES.2005.1489581.

Quattrociocchi, W., Caldarelli, G., and Scala, A. (2014). Self-healing networks: Redundancy and structure. *PLOS ONE*, 9(2), 1–7. doi:10.1371/journal.pone.0087986. URL `https://doi.org/10.1371/journal.pone.0087986`.

Rodrigues Mendes Ribeiro, R., Bessani, M., de Souza Sant Anna Fogliatto, M., and Dias Maciel, C. (2019). Resilience assessment of self-healing systems with redundancy. *IEEE Latin America Transactions*, 17(09), 1546–1551.

Shahbazian, A., Fereidunian, A., and Manshadi, S.D. (2020). Optimal switch placement in distribution systems: A high-accuracy milp formulation. *IEEE Transactions on Smart Grid*, 11(6), 5009–5018. doi:10.1109/TSG.2020.3000315.

Shen, L., Tang, Y., and Tang, L.C. (2021). Understanding key factors affecting power systems resilience. *Reliability Engineering & System Safety*, 212, 107621.

Yusta, J.M., Correa, G.J., and Lacal-Arántegui, R. (2011). Methodologies and applications for critical infrastructure protection: State-of-the-art. *Energy Policy*, 39(10), 6100 – 6119. doi:https://doi.org/10.1016/j.enpol.2011.07.010. URL `http://www.sciencedirect.com/science/article/pii/S0301421511005337`. Sustainability of biofuels.